Available online at www.sciencedirect.com
SCIENCE DIRECT®
ELSEVIER
Nuclear Instruments and Methods in Physics Research A 554 (2005) 340–346
NUCLEAR INSTRUMENTS & METHODS IN PHYSICS RESEARCH Section A
www.elsevier.com/locate/nima

A compensated fission detector based on photovoltaic cells

M. Petit[a], T. Ethvignot[a], T. Granier[a,*], R.C. Haight[b], J.M. O'Donnell[b], D. Rochman[b,1], S.A. Wender[b], E.M. Bond[c], T.A. Bredeweg[c], D.J. Vieira[c], J.B. Wilhelmy[c], Y. Danon[d]

[a]*CEA/DAM Ile-de-France, DPTA/Service de Physique Nucléaire, BP 12, 91680 Bruyères-le-Châtel, France*
[b]*LANSCE-3, Los Alamos National Laboratory, MS H855, Los Alamos, NM 87545, USA*
[c]*C-INC, Los Alamos National Laboratory, MS J514, Los Alamos, NM 87545, USA*
[d]*Rensselaer Polytechnic Institute, Troy, NY 12180, USA*

Received 27 May 2005; received in revised form 29 July 2005; accepted 28 August 2005
Available online 16 September 2005

Abstract

Standard techniques of event-by-event detection of fission may fail when operated in high γ-ray or particle radiation environments. This is the case within the 800 MeV proton-driven lead slowing-down neutron spectrometer at LANSCE where standard fission detectors are found to be inoperable for microseconds to milliseconds after each proton pulse. To overcome this problem, a simple fission fragment detector based on compensated photovoltaic cells has been developed. The compensated detector has lower susceptibility to the strong γ-flash and can recover much faster than an uncompensated detector. This detector is well adapted to applications involving the detection of fission in regions where high intensity γ-ray and/or particle radiation fields exist.

Keywords: Fission; Fission detection; Compensated detector; Lead slowing-down spectrometer; Photovoltaic cells

1. Introduction

A lead slowing-down spectrometer (LSDS) has been recently implemented on the 800 MeV proton beam line of the Los Alamos Neutron Science Center (LANSCE) with the ultimate goal of measuring the neutron-induced fission cross-section of the first metastable state of uranium 235 (^{235m}U, 77 eV) in the 1 eV–100 keV region [1]. This unprecedented measurement will provide new constraints to the nuclear reaction models which predict substantial differences between the isomer and the ground state cross-sections. Indeed, in this energy domain, one expects a cross-section up to

*Corresponding author. Tel.: +33 1 6926 5786; fax: +33 1 6926 7663.
E-mail address: thierry.granier@cea.fr (T. Granier).
[1]Present address: National Nuclear Data Center, Brookhaven National Laboratory, Upton, NY 11973-5000, USA.

0168-9002/$ - see front matter © 2005 Elsevier B.V. All rights reserved.
doi:10.1016/j.nima.2005.08.093

40% smaller for the excited state [2,3] whereas at thermal energy previous measurements have reported an isomeric cross-section that is twice as large as that for the ground state [4–6].

Since the half-life of ^{235m}U is relatively short (26 min), only small samples, i.e. ~10 nanograms, will be available. To compensate for the limitation in count rate, the main advantage of the new proton-driven lead spectrometer is to provide an intense neutron flux in the 1 eV–100-keV region. The instrument consists of a 20 metric tonne cubic lead assembly to the center of which the LANSCE proton storage ring 800 MeV proton beam is transported and stopped in a tungsten target. The proton beam is emitted within short pulses (typically <200 ns) and induces spallation reactions in the tungsten target. Most of the neutrons resulting from these reactions slow down through multiple, quasi-isotropic elastic scattering in the lead assembly from the MeV region down to the thermal regime, giving the system its properties of spectrometry and high neutron intensity [7]. Detailed descriptions of the instrument's characteristics and the experimental program are given in Ref. [1] as well as references of previous works that have lead to this established technique.

To perform the detection and counting of fission, thin photovoltaic cells (often referred to as solar cells) used as fission fragment detectors are one of the options followed in our experimental program. These detectors are compact, rugged and inexpensive and they have a high efficiency (see e.g. Refs. [8,9]). Nevertheless, with increasing proton pulse power in the LSDS, solar cells as well as other classical detectors (i.e., ionization chambers, surface barrier junctions, scintillators, etc.) are subject to oscillation and saturation due to the interaction with the intense high energy particles and prompt γ-rays accompanying the spallation reactions (γ-flash). This results in a dead time after each proton pulse and this makes detection of fission very difficult or impossible. Indeed, the net effect is a loss of fission events affecting the higher energy part of the neutron spectrum which corresponds to the shorter time-of-flight. This problem required implementing a compensated detector system similarly to what is classically done with ionization chambers used in high γ-ray fluxes.

2. Solar cells as fission detectors in a LSDS

The use of solar cells as fission fragment detectors is a well-known technique in experimental nuclear physics (see for example Refs. [10,11]).

In our experimental program we aim at measuring the fission cross-section of ^{235m}U and other rare isotopes relative to ^{235}U. The absolute determination of the detection efficiency is thus not required. In this framework, photovoltaic cells offer several advantages. They can operate in open air and are quite insensitive to radiation damage. Their mass is relatively small and therefore, they induce minimal perturbations on the neutron flux. Also, as they do not require vacuum pumping, so operations with fissile samples are more rapid and convenient than with the usual ionization fission chambers. This point is particularly important in the case of short-lived nuclei such as ^{235m}U.

The thin (~140 μm, solar cells used in this work were developed for the space industry [12]. They are $2 \times 2\,cm^2$ Si junctions with one side covered with a silver backing. Their full characteristics as fission fragment detectors (i.e. timing, detection efficiency, Schmitt parameters, etc.) are summarized in Ref. [8].

For the tests in the LSDS, we used long-lived fissionable material such as ^{235}U and ^{239}Pu. The samples were deposited directly onto the active surface by electrodeposition. Alternatively, they can be deposited on a separate substrate and brought next to the detector for fission counting.

The cells are operated with the "SAPhIR" preamplifier that were specially developed with surface mounted component technology for use with photovoltaic cells used as fission detectors [13]. This preamplifier is adapted to the cells' large intrinsic capacity (several nF/cm^2). The output voltage is linearly proportional to the input current. The fast intrinsic rise time (~10 ns) is therefore preserved. The typical pulse height for fission fragments is 50 mV with 10 mV of white noise (for a $2 \times 2\,cm^2$ cell). The decay time constant is about 500 ns.

In this work, the fission cross section measurements solely require timing information from the fission pulses out of the preamplifier. Discrimination from noise was achieved either with classical electronics (fast filter amplifier and constant fraction discriminator) or through digital filtering algorithms (see Ref. [14]).

3. γ-Flash saturation

The γ-flash effect is strongly correlated with the number of protons per beam pulse. The experiments with ^{235m}U will necessitate a proton integrated intensity of 1 μA. With the usual proton storage ring (PSR) repetition rate of 20 Hz, this corresponds to proton pulses of 50 nC integrated charge. However, ongoing developments will allow the PSR to be operated at 30 Hz and possibly at 40 Hz allowing to lower the beam pulse size to respectively 33 and 25 nC/pulse. In practice, the γ-flash effect depends also on the position within the lead assembly. We observed that the effect decreases when the distance to the target is increased. Also, it is more pronounced in the downstream part of the assembly.

Typical waveforms exhibiting ringing and saturation are plotted in Fig. 1 for three different sizes of the proton pulses. They correspond to the voltage output of the preamplifier recorded after the proton pulse (at $t = 0$). The detector was located at a distance of ~60 cm from the center of the assembly. In each case, shortly after the proton pulse, one can observe a high amplitude signal attributed to the γ-flash (1). This signal is followed in Fig. 1(a) and (b) by a ringing with ~25 μs period (2). Only the positive excursions are visible since the preamplifier output saturates at negative values (~ -90 mV with a 1 MΩ impedance). The same ringing also exists for higher numbers of protons per pulse (Fig. 1(c)), but it is preceeded by a long negative period of saturation (7). The total duration of the saturation and ringing can reach several milliseconds depending on the number of protons in the beam pulse. It is then followed by a return to the baseline (3). Fission signals are visible (arrows) on top of the γ-flash signal and after the ringing (4). They are also observed on top of the ringing (6) and in the saturation region between two positive excursions (5). In these cases there is no time dependent inefficiency in the detection of fission provided that the subsequent signal processing is able to discriminate the fission signals [14].

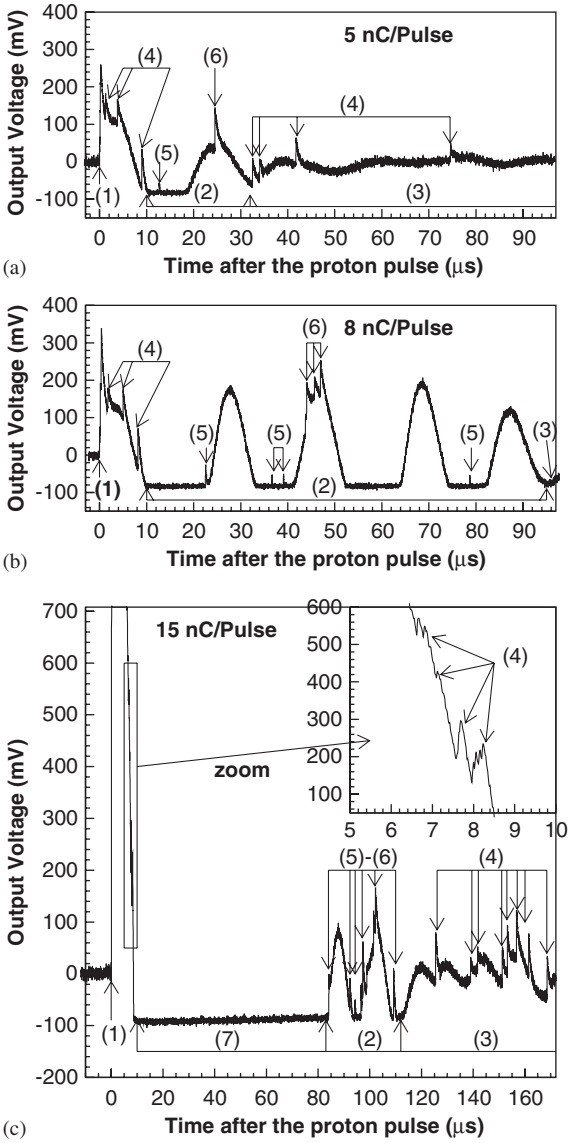

Fig. 1. Waveforms (output voltage as a function of time) recorded after one proton pulse with a ^{235}U coated solar cell (without compensation) in the LSDS, for 3 different proton pulse sizes: 5 nC (a), 8 nC (b) and 15 nC (c). Time 0 corresponds to the incident proton pulse. Fission signals are indicated by arrows (see text for additional discussion).

However, in the case of Fig. 1(c), no fission is observed in the first saturation period (7), i.e. for 80 μs after the beam pulse emission. This corresponds to neutron energies higher than ~25 eV. Thus, for 15 nC proton pulses no cross-section measurement is possible above ~25 eV no matter of the level of performance of signal processing. Tests at higher proton pulse intensity confirm the irreversible loss of the fission events for even larger periods after the proton pulse, i.e. at lower neutron energy.

In order to extend the range of fission detection up to 100 keV, one must be able to recover from the saturation in less than a microsecond. For this purpose, a method of γ-compensation for solar cells was developed similarly to the 50-year-old technique of γ-compensated ionization chambers [15,16]. The technique was tested at ELSA, a pulsed γ-ray source facility at Bruyères-le-Châtel [17,18] and directly within the LSDS at LANSCE.

4. γ compensation with solar cells

The compensation principle proposed here is based on two identical solar cells that are connected together so that their current outputs are opposite. One of the cells is exposed to the fissile sample and is used as a fission fragment detector. The other cell is not exposed to the fission source and serves as a compensator. As both cells experience the same γ-flash, γ-flash-induced signals compensate whereas the fission signals are preserved. Two basic diagrams follow this principle with the cells connected either in antiparallel or in antiseries. In this work the antiparallel connection was used. The compensated setup is sketched in Fig. 2. Although this connection alters slightly the signal to noise ratio with the Saphir preamplifier, it was checked with a spontaneous fission source (^{252}Cf) that the detection efficiency, timing and response linearity were preserved.

In order to test the response of the compensated setup to a γ-flash, photon irradiations have been performed at the ELSA facility. The photon beams were produced by Bremmstrahlung by bombarding a 1.2 mm Ta converter with a

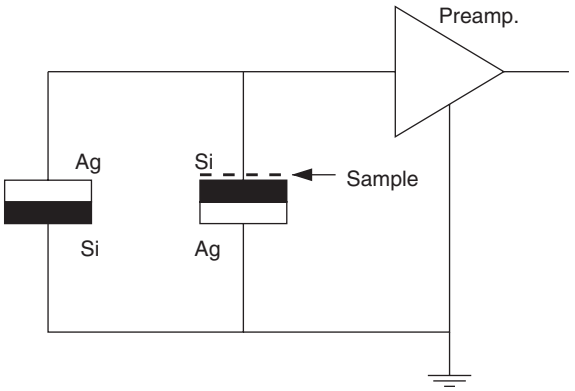

Fig. 2. Diagram of the compensated fission detector. The cells are connected in antiparallel order to compensate (by subtraction) the signals induced by the γ-flash.

15 MeV electron beam. The electron pulses were Gaussian (150 ns FWHM) and were delivered at a 10 Hz repetition rate. The solar cell setup was placed 150 cm downstream to the target. No fissionable samples were used in these tests. Fig. 3 represents the setup response with and without compensation. The number of beam electrons per pulse was increased by a factor of four for the experiment with compensation in order to evaluate the effect with greater sensitivity. Thus an attenuation by a factor of 20 is observed on the γ-flash-induced signal with this simple compensation system. This prevents the preamplifier from saturating and oscillating.

The compensated setup has also been tested in the LSDS with fissionable samples. Similar compensation performance was obtained, i.e. reduction of the γ-flash signal over the whole time range. This is illustrated at Fig. 4 where a waveform obtained with a 40 nC proton pulse is displayed. One can note that the amplitude of the excursions near $t = 0$ are largely reduced compared to Fig. 1(c). Also, no saturation is observed and the fission signals are easily distinguished on top of the distorted base line. The fission signals were discriminated online through signal processing and we were able to achieve satisfactory measurements of standard cross sections up to neutron energies of 50 keV (i.e. down to ~1.5 μs after the proton pulse) with 40 nC proton pulses.

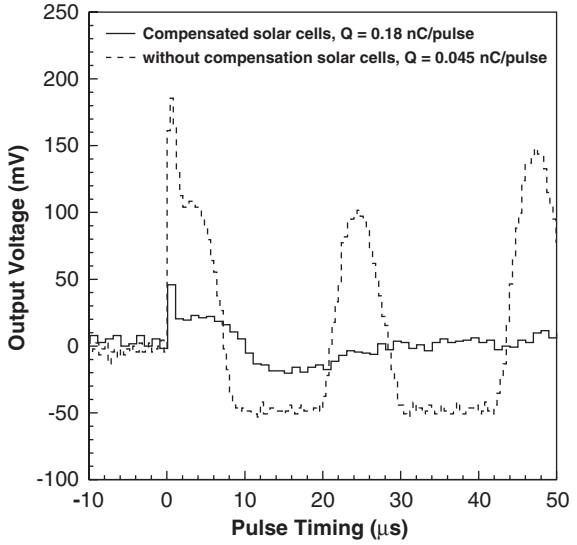

Fig. 3. Response to a γ-flash (at $t = 0$) with (full line) and without (dashed line) compensation (identical cells, no fissionable material). Note that the electron beam intensity was larger by a factor of 4 in the case of compensated setup: 0.18 vs. 0.045 nC/pulse. Therefore, the compensation reduced the γ-flash peak by a factor of 20.

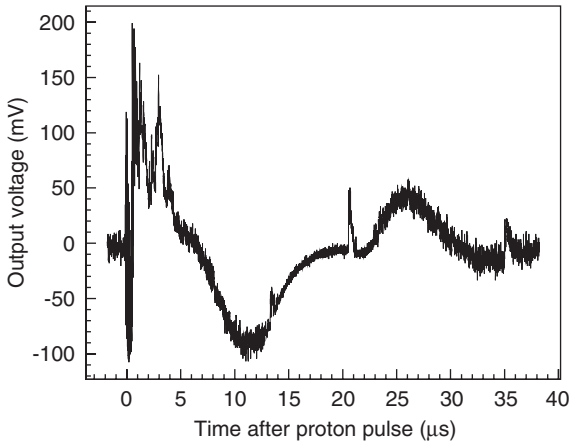

Fig. 4. Waveform obtained in the LSDS with the compensated setup in the case of a 40 nC proton pulse (preamplifier output). The amplitude of the excursions near $t = 0$ is drastically reduced compared to Fig.1(c) and fission signals are observed.

5. Investigations towards a refined compensation

Small compensation defects may remain however, due to small differences in the cells' susceptibility. The compensation level can be improved by adjusting the cells response to the γ-flash until they match and cancel precisely. This can be obtained through a divider bridge with a variable potentiometer such as in the diagram represented in Fig. 5. With this diagram, a compensation refinement is possible only if the intrinsic sensitivity of the compensating cell is slightly higher than the sensitivity of the compensated cell. This can be obtained by reducing the size of the compensating cell (by cutting out a small fraction of it) which then gets a smaller capacitance. Then the refined compensation is reached by adjusting the potentiometer. Fig. 6 represents output signals obtained at ELSA with the compensated setup for four different values of the potentiometer (0, 20, 50 and 325 Ω) in response to equivalents γ-flashes. The best compensation was obtained for a 20 Ω resistance. For a null resistance, i.e. no divider bridge, the resulting signal was found negative due to the slightly larger intrinsic sensitivity of the compensating cell. In the future, this system will be equipped with a motorized potentiometer so that the compensation level may be remotely optimized.

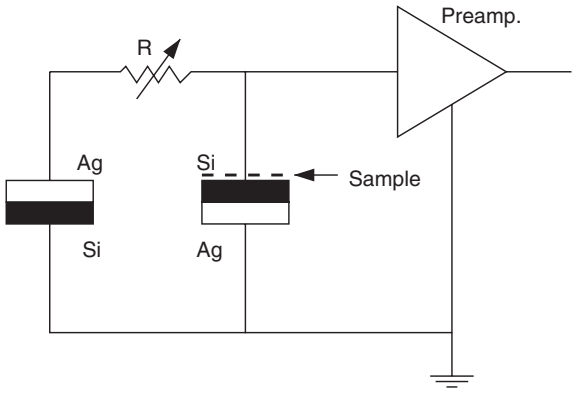

Fig. 5. Diagram of a refined compensation system. A potentiometer R is inserted between the two cells.

6. Conclusion

A compensated fission detector based on photovoltaic cells has been designed for operation at the 800 MeV proton-driven lead slowing-down

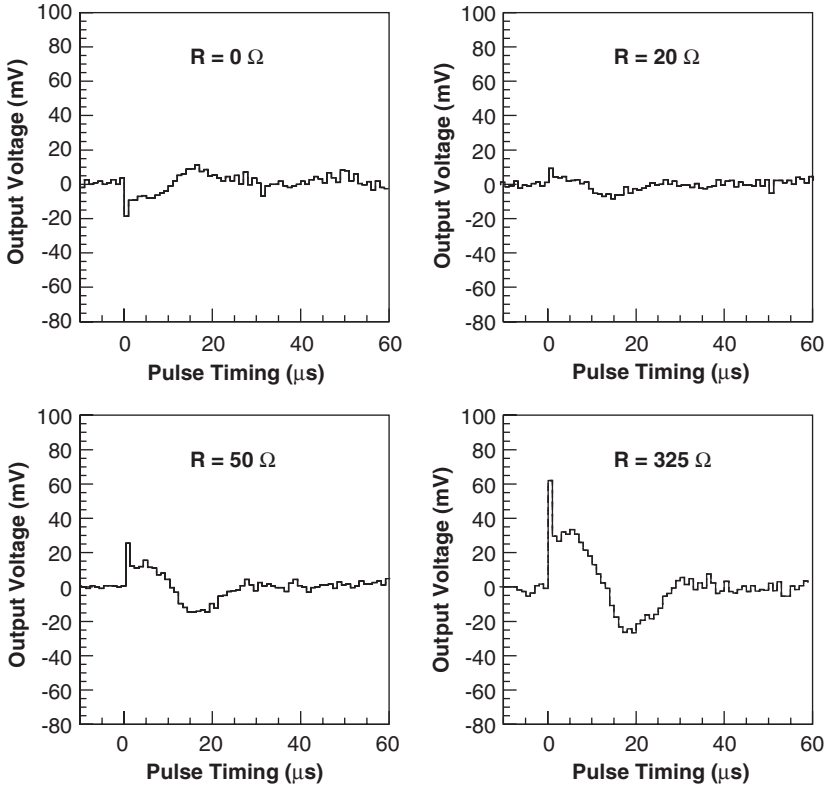

Fig. 6. Response of the compensated solar cell to the same γ-flash with four different values of the potentiometer. In order to perform a fine adjustment, the compensating cell had a slightly higher gain than the compensated cell. Therefore, the signal is negative for $R = 0\,\Omega$.

spectrometer at LANSCE. The detector is designed so that the γ-flash induced signal is dramatically reduced before preamplification. We have demonstrated this method with success in the LSDS for proton intensities up to 40 nC/pulse which is above the beam pulse size required for the future experiments with 1 μA proton integrated intensity and 30 Hz repetition rate. Investigations are in progress to extend this domain of operation to larger beam pulse sizes in the near future. They focus on compensation refinement, preamplifier optimization and waveform digital filtering.

This detector should also be useful for other applications, in particular where the detection of fission within high radiation environments is involved.

References

[1] D. Rochman, R.C. Haight, J.M. O'Donnell, A. Michaudon, D.J. Vieira, E.M. Bond, T.A. Bredeweg, A. Kronenberg, J.B. Wilhelmy, T. Ethvignot, T. Granier, M. Petit, Y. Danon, Nucl. Instr. and Meth. A (2005), accepted for publication.
[2] J.E. Lynn, A.C. Hayes, Phys. Rev. C 67 (2003) 014607.
[3] W. Younes, H.C. Britt, Phys. Rev. C 68 (2003) 034610.
[4] V.I. Mostovoi, G.I. Ustroyev, At. En. 5 (1964) 241.
[5] W. Talbert, et al., Phys. Rev. C 36 (1987) 1896.
[6] A. D'Eer, et al., Phys. Rev. C 38 (1988) 1270.
[7] T. Granier, L. Pangault, T. Ethvignot, R.C. Haight, X. Ledoux, V. Méot, Y. Patin, P. Pras, M. Szmigiel, R.S. Rundberg, J.B. Wihelmy, Nucl. Instr. and Meth. A 506 (2003) 149.
[8] T. Ethvignot, T. Granier, L. Giot, P. Casoli, R.N. Nelson, Nucl. Instr. and. Meth. A 490/3 (2002) 559.
[9] M. Petit, Thèse de doctorat, Université de Bordeaux, France, 2002.

[10] G. Siegert, Nucl. Instr. and Meth. A 164 (1979) 437.
[11] E. Liatard, et al., Nucl. Instr. and Meth. A 267 (1988) 231.
[12] The thin solar cells were purchased from Solar World (http:www.solar-world.com).
[13] C.H. Theisen, et al., A fission-fragments detector, in: Proceedings of the Second International Workshop on Nuclear Fission and Fission-Product Spectroscopy, Seyssins, France, 22–25 April 1998, AIP, New York, NY, 1998, p. 143.
[14] K.D. Huff, Digital filtering applications to the lead slowing-down spectrometer, Los Alamos National Laboratory Report LA-UR-04-8757, 2004.
[15] D.H. Wilkinson, Ionization Chambers and Counters, Cambridge University Press, Cambridge, 1950.
[16] P.E. Koehler, J.A. Harvey, N.W. Hill, Nucl. Instr. and Meth. A 361 (1995) 270.
[17] J.-G. Marmouget, A. Binet, Ph. Guimbal, J.-L. Coacolo, Present performance of the low-emittance, high-bunch charge ELSA photo-injected Linac, in: EPAC'02 Proceedings, Paris, 2002, p. 1795, http://accelconf.web.cern.ch/Accelconf/e02.
[18] Ph. Guimbal, et al., Status of the ELSA-2 project, in: EPAC'02 Proceedings, Paris, 2002, p. 1768, http://accelconf.web.cern.ch/Accelconf/e02.